Review Article

Diffusion Tensor Imaging of Cerebral White Matter: A Pictorial Review of Physics, Fiber Tract Anatomy, and Tumor Imaging Patterns

Brian J. Jellison, Aaron S. Field, Joshua Medow, Mariana Lazar, M. Shariar Salamat, and Andrew L. Alexander

We review the normal anatomy of the white matter (WM) tracts as they appear on directional diffusion tensor imaging (DTI) color maps, which will almost certainly be available to the general radiologist as part of a commercial DTI software package in the near future. Anatomic drawings and gross dissection photographs are correlated with the directional DTI color maps to review the anatomy of those tracts readily seen in most cases. We also include several correlative examples of so-called tractograms in which specific tracts are traced and displayed by using computer-graphical techniques (1). Since several excellent reviews focusing on tractography and other sophisticated DTI postprocessing techniques are already published (2–4), we focus on the directional eigenvector color maps. A brief review of the basic principles underlying DTI is also included; several more comprehensive reviews are available for the reader who wishes to delve deeper into the technical aspects of DTI (5, 6). Finally, we briefly review the DTI patterns that result when a cerebral neoplasm involves WM tracts; knowledge of these patterns becomes critically important when neurosurgeons use DTI in planning tumor resections, as they frequently do at our institution (7, 8).

The Physics of DTI

By applying the appropriate magnetic field gradients, MR imaging may be sensitized to the random, thermally driven motion (diffusion) of water molecules in the direction of the field gradient. Diffusion is *anisotropic* (directionally dependent) in WM fiber tracts, as axonal membranes and myelin sheaths present barriers to the motion of water molecules in directions not parallel to their own orientation. The direction of maximum diffusivity has been shown to coincide with the WM fiber tract orientation (9). This information is contained in the *diffusion tensor*, a mathematic model of diffusion in three-dimensional space. In general, a *tensor* is a rather abstract mathematic entity having specific properties that enable complex physical phenomena to be quantified. In the present context, the tensor is simply a matrix of numbers derived from diffusion measurements in several different directions, from which one can estimate the diffusivity in *any arbitrary direction* or determine the direction of maximum diffusivity.

The tensor matrix may be easily visualized as an *ellipsoid* whose diameter in any direction estimates the diffusivity in that direction and whose major principle axis is oriented in the direction of maximum diffusivity (Fig 1) (10). With use of DTI, both the degree of anisotropy and the local fiber direction can be mapped voxel by voxel, providing a new and unique opportunity for studying WM architecture in vivo.

The tensor model of diffusion consists of a 3×3 matrix derived from diffusivity measurements in at least six noncollinear directions. The tensor matrix is diagonally *symmetric* ($\mathbf{D}ij = \mathbf{D}ji$) with six degrees of freedom (ie, only six of the tensor matrix's nine entries are independent and so the matrix is fully determined by these six parameters), such that a minimum of six diffusion-encoded measurements are required to accurately describe the tensor. Using more than six encoding directions will improve the accuracy of the tensor measurement for any arbitrary orientation (11–13).

The tensor matrix is subjected to a linear algebraic procedure known as *diagonalization*, the result of which is a set of three *eigenvectors* representing the major, medium, and minor principle axes of the ellipsoid fitted to the data and the corresponding three *eigenvalues* ($\lambda_1, \lambda_2, \lambda_3$), which represent the apparent diffusivities along these axes. (The word *eigen* is Germanic in origin, meaning "peculiar" or "special." The term *eigenvalue* was used by British algebraists in the late 19th century to refer to a "characteristic value" of a matrix; specifically, a number k is called an *eigenvalue* of the matrix $\mathbf{A}$ if there exists a nonzero vector $\mathbf{v}$ such that $\mathbf{Av} = k\mathbf{v}$. In this case, the vector $\mathbf{v}$ is called
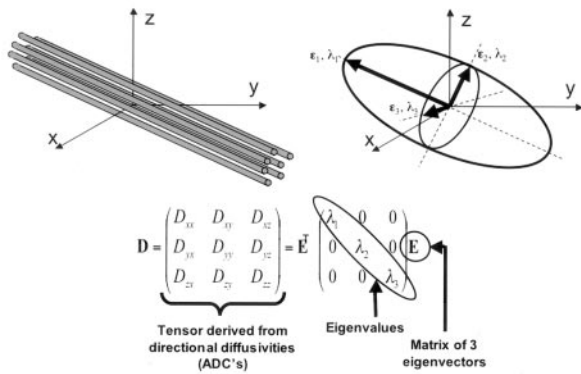
FIG 1. *Top left*, Fiber tracts have an arbitrary orientation with respect to scanner geometry (*x, y, z* axes) and impose directional dependence (anisotropy) on diffusion measurements.

Top right, The three-dimensional diffusivity is modeled as an ellipsoid whose orientation is characterized by three eigenvectors (ϵ_1, ϵ_2, ϵ_3) and whose shape is characterized three eigenvalues (λ_1, λ_2, λ_3). The eigenvectors represent the major, medium, and minor priniciple axes of the ellipsoid, and the eigenvalues represent the diffusivities in these three directions, respectively.

Bottom, This ellipsoid model is fitted to a set of at least six noncollinear diffusion measurements by solving a set of matrix equations involving the diffusivities (*ADC's*) and requiring a procedure known as matrix diagonalization (12, 18). The major eigenvector (that eigenvector associated with the largest of the three eigenvalues) reflects the direction of maximum diffusivity, which, in turn, reflects the orientation of fiber tracts. Superscript *T* indicates the matrix transpose.

an *eigenvector* of **A** corresponding to *k* [14].) This procedure may be thought of as a rotation of the *x, y,* and *z* coordinate system in which the data were acquired (dictated by scanner geometry) to a new coordinate system whose axes are dictated by the directional diffusivity information (Fig 1).

Diffusion anisotropy is easily understood as the extent to which the shape of the tensor ellipsoid deviates from that of a sphere; mathematically, this translates to the degree to which the three tensor eigenvalues differ from one another. Any of several anisotropy metrics may be used, one of the most

common being *fractional anisotropy* (FA) (15), which derives from the standard deviation of the three eigenvalues and ranges from 0 (isotropy) to 1 (maximum anisotropy):

1)

$$FA = \sqrt{\frac{3}{2}} \sqrt{\frac{(\lambda_1 - \bar{\lambda})^2 + (\lambda_2 - \bar{\lambda})^2 + (\lambda_3 - \bar{\lambda})^2}{\lambda_1^2 + \lambda_2^2 + \lambda_3^2}}$$

where $\bar{\lambda}$ denotes the mean of the three eigenvalues, which is equal to the directionally averaged diffusivity. The direction of maximum diffusivity may be mapped by using red, green, and blue (RGB) color channels with color brightness modulated by FA, resulting in a convenient summary map from which the degree of anisotropy and the local fiber direction can be determined (Fig 2) (16).

Methods

DTI MR Acquisition and Directional Mapping

DTI MR images for this review were obtained with a 1.5-T system (GE Medical Systems, Milwaukee, WI) by using a quadrature birdcage head coil, single-shot echo planar imaging sequence (4500/71.8/4 [TR/TE/excitations], 240-mm field of view, 3-mm sections, 2 slabs, 20 sections per slab), matrix 128 × 128 zero-filled to 256 × 256, voxel size 1.87 × 1.87 × 3.0 mm interpolated to 0.94 mm isotropic, diffusion encoding in 23 directions (minimum energy optimization [12]) with b = 0, 1000 s/mm², postprocessing with Automated Image Registration (17), a 3 × 3 in-plane spatial median filter, tensor decoding and diagonalization (12, 18). The choice of 23 directions represented a somewhat arbitrary balance between accuracy in fitting the tensor model (increasing the number of encoding directions decreases the variance in the tensor model parameters) and the number of sections that could be acquired (our imaging system limits the number of images per series to 512). The eigenvalues and eigenvectors of the diffusion tensor
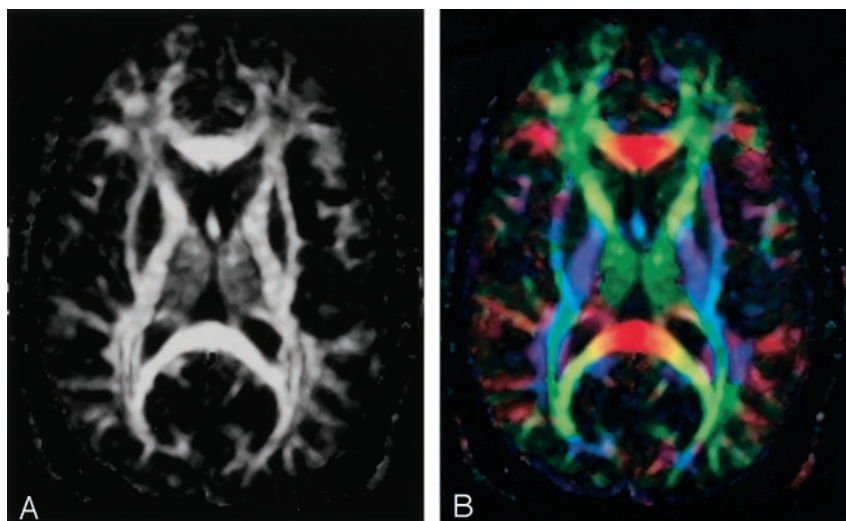

FIG 2. *A,* FA map without directional information.

B, Combined FA and directional map. Color hue indicates direction as follows: red, left-right; green, anteroposterior; blue, superior-inferior. This convention applies to all the directional maps in this review. Brightness is proportional to FA.
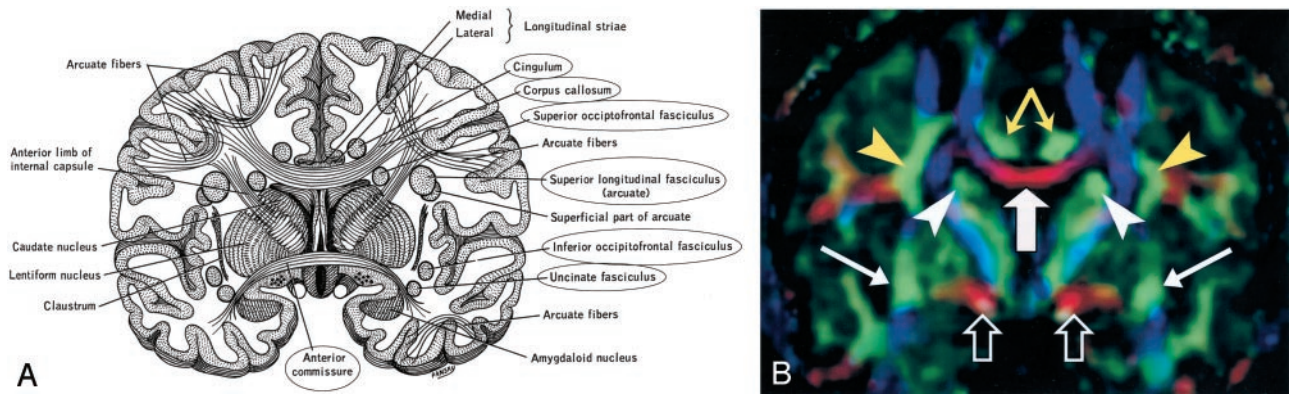
FIG 3. *A*, Illustration shows the anatomic relationships of several WM fiber tracts in the coronal plane. Circled tracts are those further illustrated in this review. The corpus callosum is "sandwiched" between the cingulum superomedially and the superior occipitofrontal fasciculus inferolaterally. The superior longitudinal fasciculus sweeps along the superior margin of the claustrum in a great arc. The inferior occipitofrontal fasciculus lies along the inferolateral edge of the claustrum. (Reproduced with permission from reference 20.)

B, Directional map corresponding to *A*. The paired cingula are easily identified in green (yellow arrows) just cephalad to the red corpus callosum (thick white arrow). White arrowheads indicate superior occipitofrontal fasciculus; thin white arrows, inferior occipitofrontal fasciculus; yellow arrowheads, superior longitudinal fasciculus. Like the corpus callosum, the commissural fibers of the anterior commissure are left-right oriented toward the midline, resulting in the characteristic red (open arrows) on this DTI map. Further lateral, the fibers diverge and mingle with other tracts; they are no longer identifiable with DTI, but can be traced with tractography.
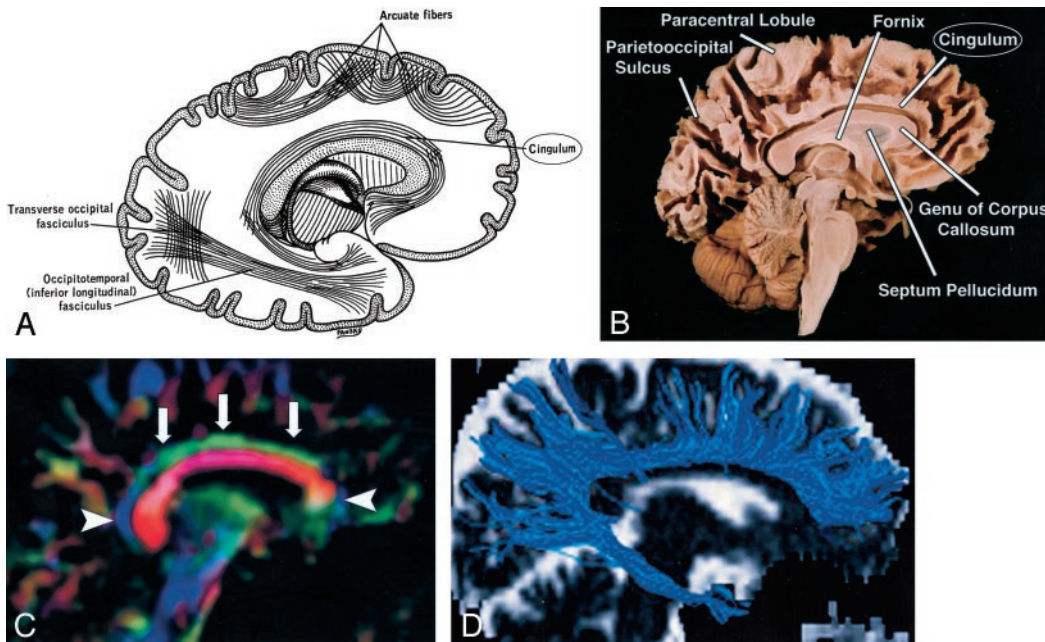

FIG 4. Cingulum, sagittal view.

A, Illustration shows the cingulum arching over the corpus callosum.

B, Gross dissection, median view.

C, Directional map. Because DTI reflects tract orientation voxel by voxel, the color changes from green to blue as the cingulum (arrows) arches around the genu and splenium (arrowheads). Green indicates anteroposterior; red, left-right; blue, superior-inferior.

D, Tractogram. (See also Fig 5A, axial directional map.)

were used to calculate maps of the diffusion tensor trace, FA, and vector orientation maps, which were generated by mapping the major eigenvector directional components in *x*, *y*, and *z* into RGB color channels and weighting the color brightness by FA. The convention we used for directional RGB color mapping is red for left-right, green for anteroposterior, and blue for superior-inferior.

DTI Tractograms

The WM tracts were estimated with tractography by using the previously described tensor deflection (TEND) algorithm (19). Tracking was initiated from a start location (or seed point) in both forward and backward directions defined by the major eigenvector at the seed point. The propagation was termi-
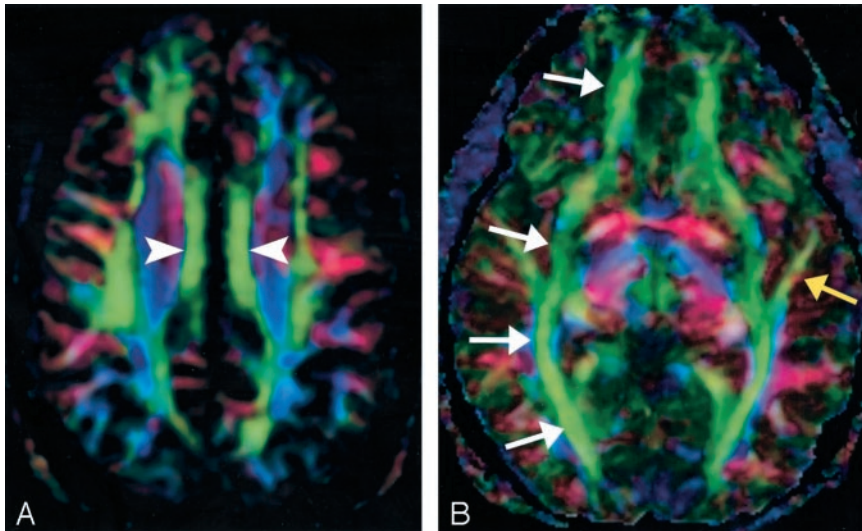
Fig 5. *A,* Cingulum, axial directional map. The paired cingula (arrowheads) are easily identified in green on this section obtained just cephalad to the corpus callosum.

B, Inferior occipitofrontal fasciculus (white arrows) and inferior longitudinal fasciculus (yellow arrow), axial directional map. The inferior occipitofrontal fasciculus lies in a roughly axial plane and is easily identified in green; it connects frontal and occipital lobes at the level of the midbrain. Posteriorly, the inferior occipitofrontal fasciculus mingles with the inferior longitudinal fasciculus, optic radiations, superior longitudinal fasciculus, and other fibers to form the sagittal stratum—a vast and complex bundle that connects the occipital lobe to the rest of the brain.
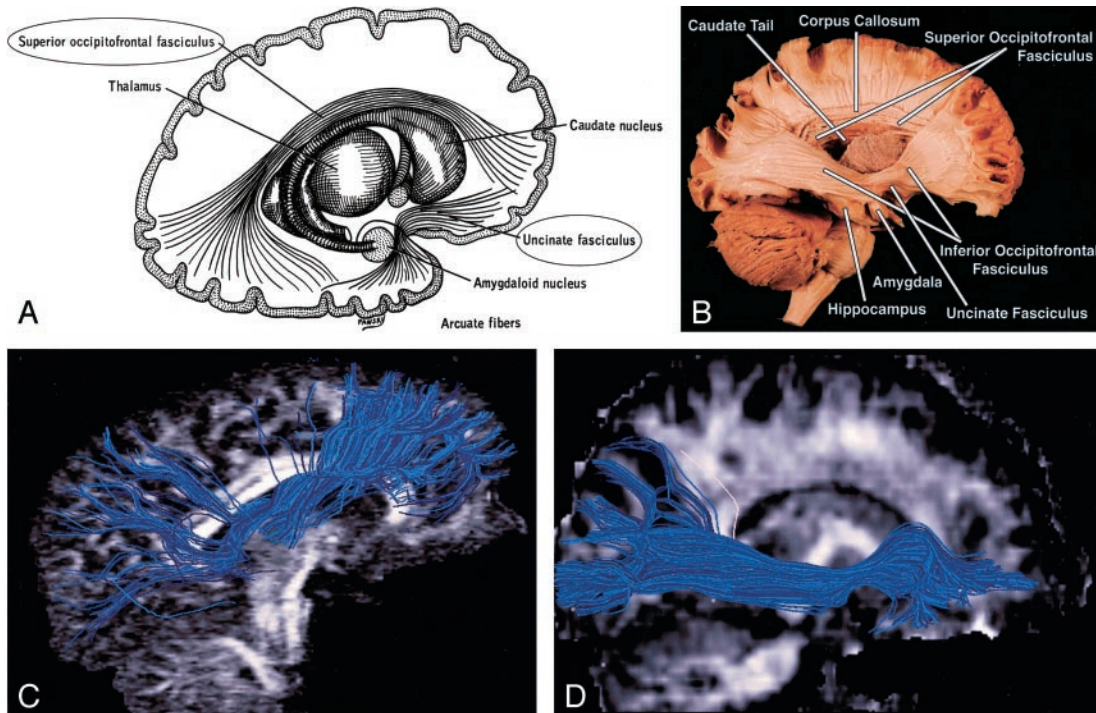

Fig 6. Superior and inferior occipitofrontal fasciculi and uncinate fasciculus, sagittal view.

A, Illustration shows the superior occipitofrontal fasciculus arching over the caudate nucleus to connect frontal and occipital lobes, and the uncinate fasciculus hooking around the lateral sulcus to connect inferior frontal and anterior temporal lobes (see also uncinate fasciculus in Figs 7 and 8B).

B, Gross dissection, lateral view. Like the superior occipitofrontal fasciculus, the inferior occipitofrontal fasciculus connects the frontal and occipital lobes, but it lies more caudad, running inferolateral to the claustrum (see also Fig 5B for axial view). The middle portion of the inferior occipitofrontal fasciculus is bundled together with the middle portion of the uncinate fasciculus.

C and *D,* Tractograms of the superior (*C*) and inferior (*D*) occipitofrontal fasciculi.

nated when the tract trajectory reached a voxel with FA less than 0.2 (the estimated major eigenvector direction becomes less accurate as FA decreases and becomes very sensitive to image noise for FA less than 0.2) or when the angle between two consecutive steps was greater than 45°.

A complete set of fiber trajectories was obtained by placing seeds in all the voxels with FA greater than 0.4 (the estimation of major eigenvector direction for

voxels with FA greater than 0.4 is expected to be sufficiently accurate to yield a good estimate of local fiber direction). Estimates of white matter pathways were generated from the center of each seed voxel. A specific tract or fasciculus was separated from the complete set of trajectories by retaining those fibers that intersected predefined regions of interest (ROIs). The ROIs were chosen to enclose tract cross sections that were visible in any of the axial, sagittal,
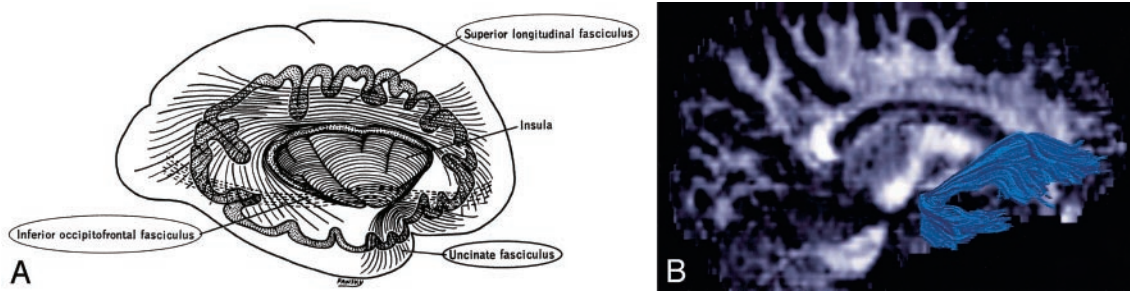
FIG 7.   Uncinate fasciculus and superior longitudinal fasciculus, sagittal view.
   A, Illustration shows the uncinate fasciculus hooks around the lateral sulcus to connect inferior frontal and anterior temporal lobes.
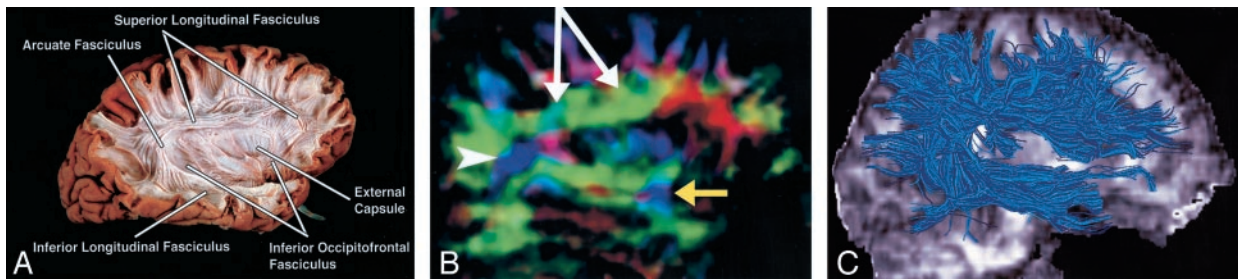   B, Tractogram. (See also Fig 6B for gross dissection.)

FIG 8.   Superior longitudinal fasciculus, sagittal view. This massive fiber bundle sweeps along the superior margin of the claustrum in a great arc. The term *arcuate fasciculus* is often used in reference to the superior longitudinal fasciculus or, specifically, its more arcuate portion.
   A, Gross dissection, lateral view.
   B, Directional map, parasagittal section. Note the color change from green to blue as the superior longitudinal fasciculus fibers turn from an anteroposterior orientation (white arrows) to a more superior-inferior orientation (arrowhead). The same phenomenon can also be seen in the uncinate fasciculus (yellow arrow).
   C, Tractogram. (See also Fig 7A.)

FIG 9.   Inferior longitudinal (occipitotemporal) fasciculus.
   A, Directional map, parasagittal section, shows the inferior longitudinal fasciculus (arrow).
   B, Tractogram. (See also Fig 8A for gross dissection and Fig 5B for axial directional map.)
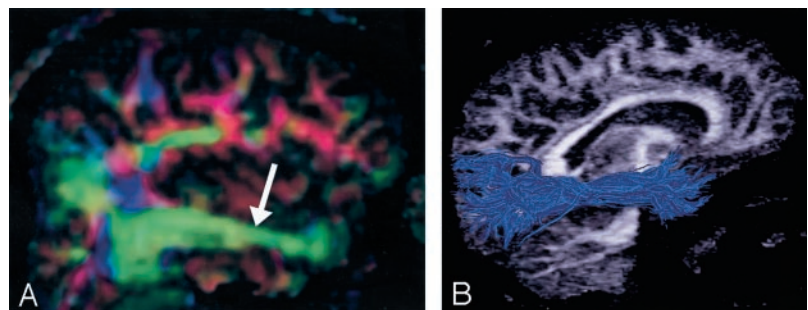
or coronal directional color maps (2, 19). Corpus callosum was selected by using the apparent tract cross section in the midsagittal plane. The anterior commissure was also selected by using an ROI placed in sagittal cross section; subsequently, only the branches that reached the temporal lobes were retained. The corticospinal tract was obtained by selecting the fibers emerging from the motor cortex and reaching the basis pedunculi. The tracts of the internal capsule were selected in an axial plane situated about halfway through the midbrain. The association fiber tracts were selected by using procedures similar to those described by Lazar et al (19).

Fiber trajectories are displayed with colors overlaid onto gray-scale anatomic images in various three-dimensional projections. Note that, unlike the directional color maps in which directional information is

color-coded, individual tractograms are displayed by using fixed colors chosen arbitrarily.

Gross Dissections

Brain specimens were removed fresh at autopsy (before fixation) and were stored in a 10% formalin bath until final preparation for dissection. Brains that were not damaged in the area of the planned dissection were rinsed for 1 hour in room- temperature tap water and then were frozen in water in a –20°C freezer for 1 week. At the end of the week, the frozen brain was rinsed with lukewarm tap water until completely thawed (about 1 hour) and then refrozen in water for another week. This process was repeated such that the brain was rinsed and thawed 3 times in total. The entire preparatory process took 3 weeks
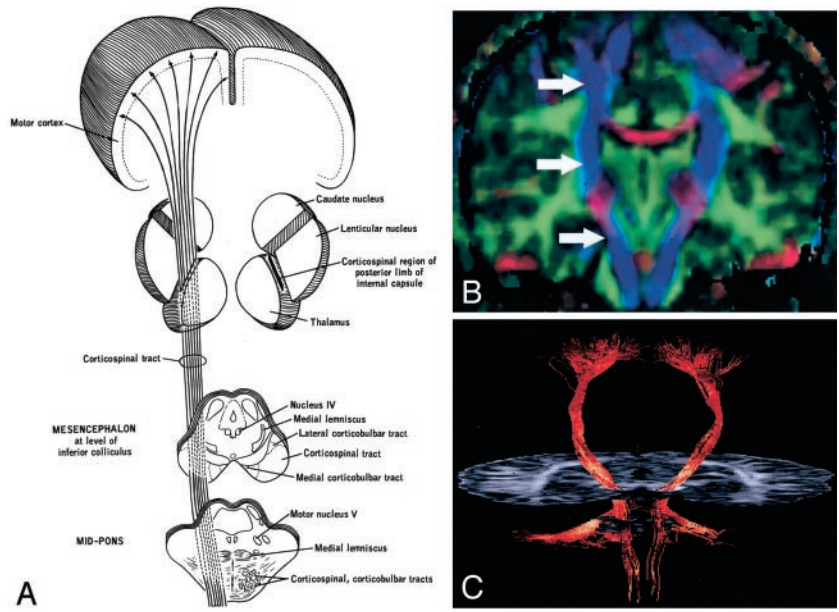
FIG 10. Corticospinal tract.

A, Illustration. (Twisting of the tract superior to the internal capsule not shown.) Corticospinal fibers originating along the motor cortex converge through the corona radiata and posterior limb of the internal capsule on their way to the lateral funiculus of the spinal cord.

B, Coronal directional map. Corticospinal fibers (arrows) are easily identified in blue on this DTI map owing to their predominantly superior-inferior orientation. The fibers take on a more violet hue as they turn medially to enter the cerebral peduncles, then become blue again as they descend through the brain stem. Corticospinal fibers run with corticobulbar and corticopontine fibers; these cannot be distinguished on directional maps but can be parsed by using tractographic techniques.
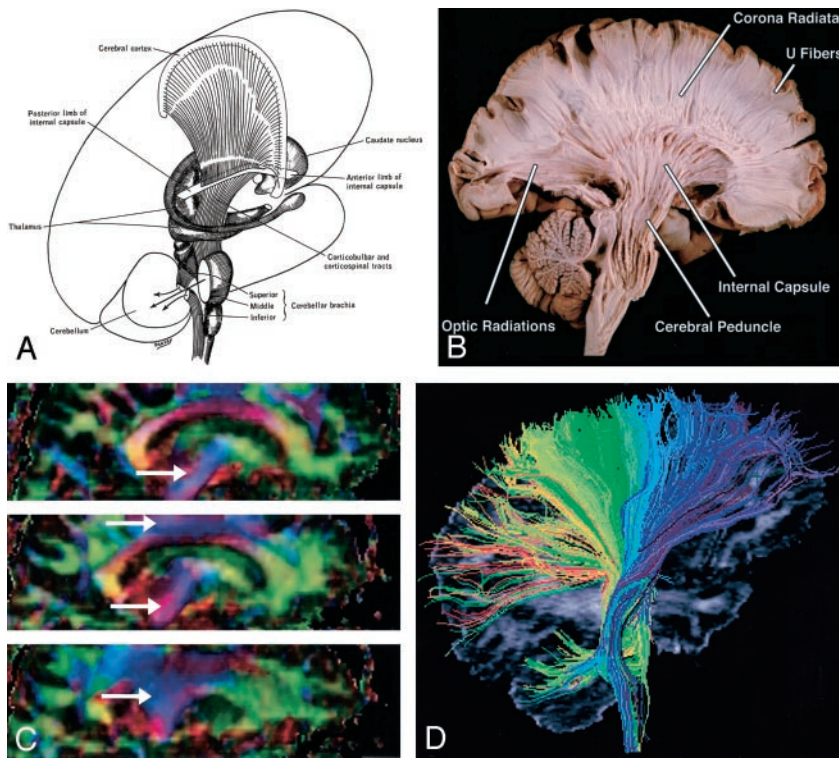
C, Tractogram.

FIG 11. *A* and *B,* Illustration (*A*) and gross dissection, medial view (*B*) of the corona radiata.

C, Directional map, three adjacent parasagittal sections, with corona radiata identifiable in blue (arrows). Corona radiata fibers interdigitate with laterally directed callosal fibers, resulting in assorted colors in the vicinity of their crossing.

D, Tractogram in which different portions of the corona radiata have been parsed by initiating the tractographic algorithm from different starting locations.

before dissection could be performed. As many dissections could not be completed in a single sitting, the unfinished specimens were placed in 5% formalin until completed, and then stored in a 10% formalin solution when done.

Illustrations

Correlative line drawings of major tracts have been reproduced from *A Functional Approach to Neuroanatomy* (20) with permission from the publisher.

WM Fiber Classification

WM fiber tracts traditionally have been classified as follows: *Association fibers* interconnect cortical areas in each hemisphere. Fibers of this type typically identified on DTI color maps include cingulum, superior and inferior occipitofrontal fasciculi, uncinate fasciculus, superior longitudinal (arcuate) fasciculus, and inferior longitudinal (occipitotemporal) fasciculus. *Projection fibers* interconnect cortical areas with deep nuclei, brain stem, cerebellum, and spinal cord. There are both efferent (corticofugal) and afferent
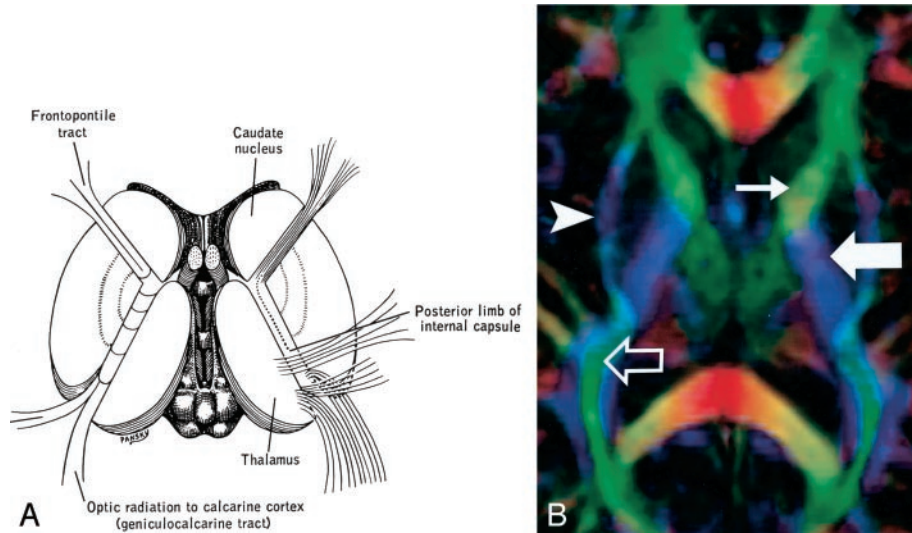
FIG 12.   Internal capsule, axial view.

A and B, Illustration (A) and directional map (B). Because the anterior limb (small arrow) primarily consists of anteroposteriorly directed frontopontine and thalamocortical projections, it appears green on this DTI map. The posterior limb (large solid arrow), which contains the superior-inferiorly directed tracts of the corticospinal, corticobulbar, and corticopontine tracts, is blue. Note also the blue fibers of the external capsule (arrowhead) and the green fibers of the optic radiations (open arrow) in the retrolenticular portion of the internal capsule.

FIG 13.   Geniculocalcarine tract (optic radiation), axial view.

A–D, Illustration (A), gross dissection (B), directional map (C), and tractogram (D). As this tract connects the lateral geniculate nucleus to occipital (primary visual) cortex, the fibers sweep around the posterior horn of the lateral ventricle and terminate in the calcarine cortex (more cephalad fibers of the optic radiation take a more direct path to the visual cortex). The optic radiation (arrows) mingles with the inferior occipitofrontal fasciculus, inferior longitudinal fasciculus, and the inferior aspect of superior longitudinal fasciculus to form much of the sagittal stratum in the occipital lobe.
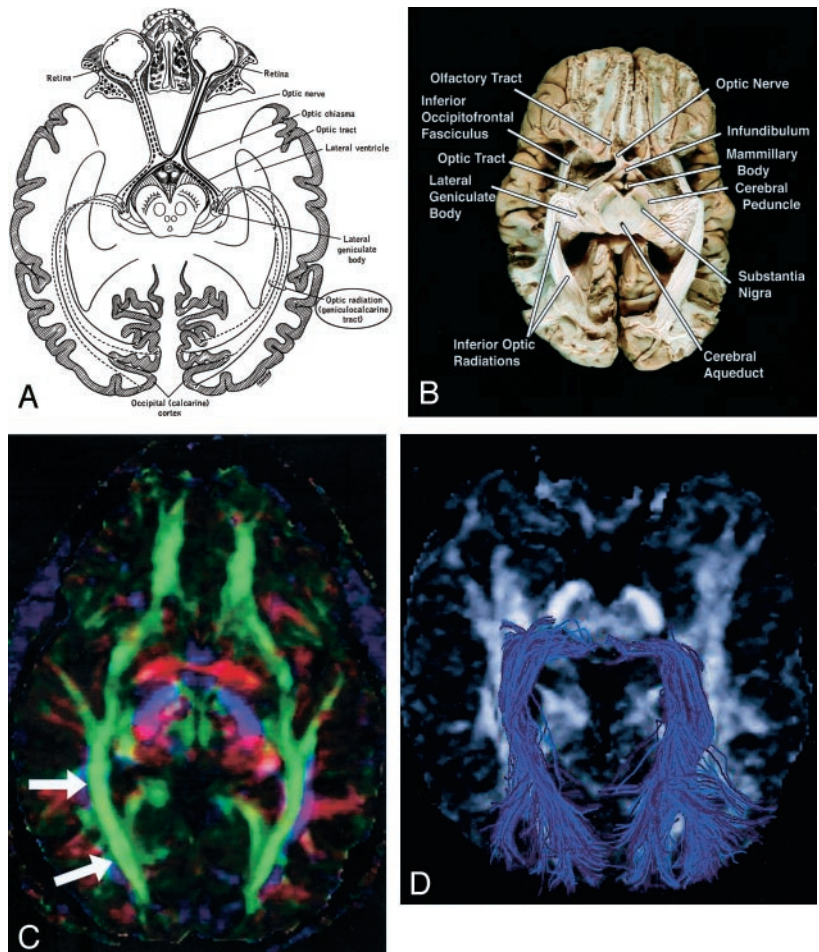
(corticopetal) projection fibers. Fibers of this type typically identified on DTI color maps include the corticospinal, corticobulbar, and corticopontine tracts, as well as the geniculocalcarine tracts (optic radiations). *Commissural fibers* interconnect similar cortical areas between opposite hemispheres. Fibers
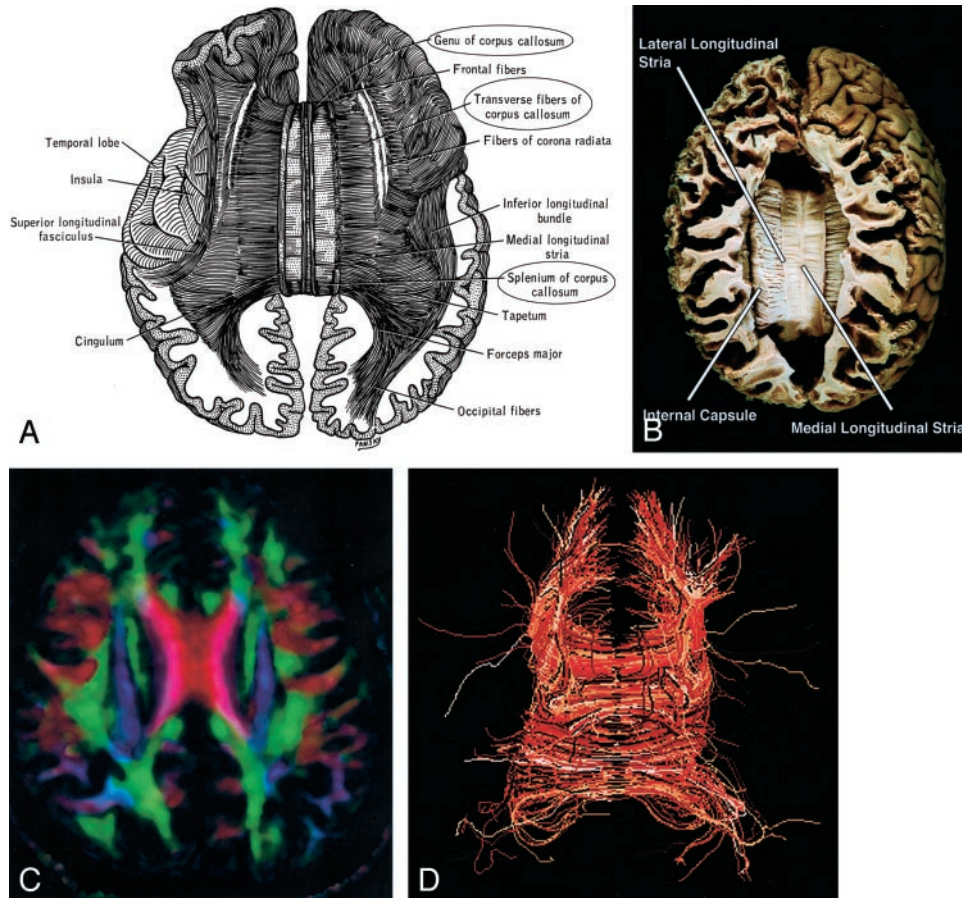
FIG 14.   Corpus callosum, axial view.

A–D, Illustration (A), gross dissection (B), directional map (C), and tractogram (D). The largest WM fiber bundle, the corpus callosum connects corresponding areas of cortex between the hemispheres. Close to the midline, its fibers are primarily left-right oriented, resulting in its red appearance on this DTI map. However, callosal fibers fan out more laterally and intermingle with projection and association tracts, resulting in more complex color patterns.
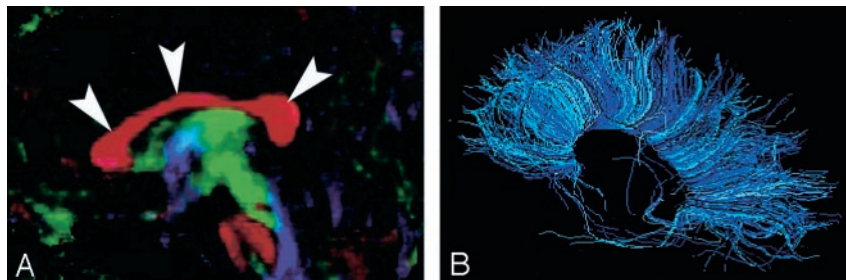

FIG 15.   A and B, Sagittal directional map of the corpus callosum (arrowheads) (A) and tractogram (B). (See also Fig 14.)

of this type typically identified on DTI color maps include corpus callosum and anterior commissure.

Other tracts that are occasionally, but not consistently, identified on directional DTI color maps include optic tract, fornix, tapetum, and many fibers of the brain stem and cerebellum. Space limitations preclude a comprehensive review of all tracts potentially visualized with DTI. Rather, we focus on the major tracts that are consistently identified in our practice.

Association Fibers

Cingulum (Figs 3, 4, and 5A).—The cingulum begins in the parolfactory area of the cortex below the rostrum of the corpus callosum, then courses within the cingulate gyrus, and, arching around the entire corpus callosum, extends forward into the parahippocampal gyrus and uncus. It interconnects portions of the frontal, parietal, and temporal lobes. Its arching course over the corpus callosum resembles the palm of an open hand with fingertips wrapping beneath the rostrum of the corpus callosum.

Superior Occipitofrontal Fasciculus (Figs 3, 6).— Whereas the cingulum wraps around the superior aspect of the corpus callosum, the superior occipitofrontal fasciculus lies beneath it. It connects occipital and frontal lobes, extending posteriorly along the dorsal border of the caudate nucleus. Portions of the superior occipitofrontal fasciculus

Fig 16. *A and B*, Axial illustration (*A*) and directional map (*B*) of the rostral midbrain.
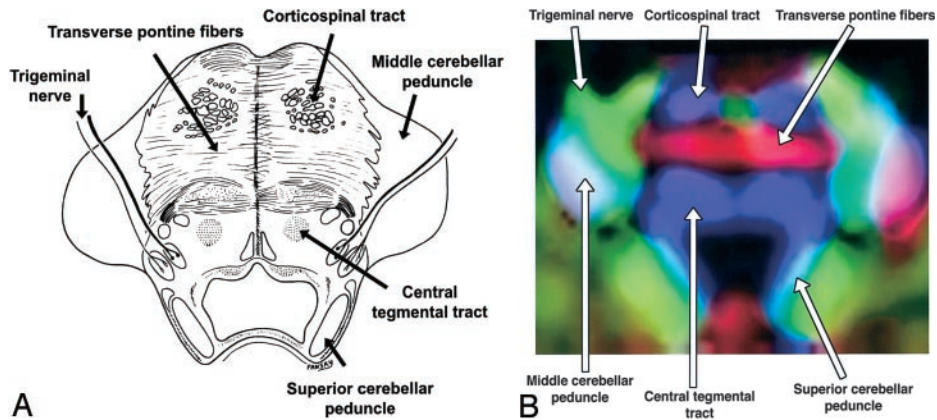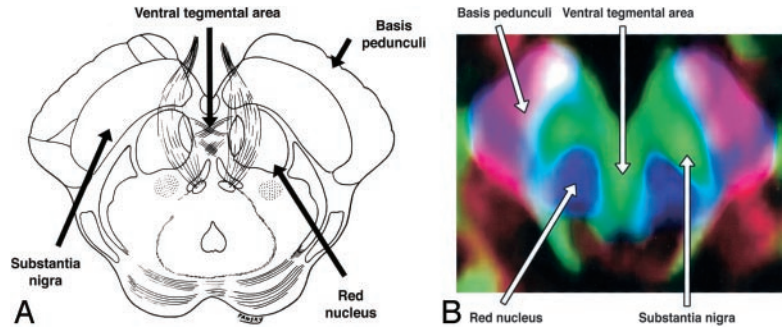
Fig 17. *A and B*, Axial illustration (*A*) and directional map (*B*) of the midpons.

parallel the superior longitudinal fasciculus (see below), but they are separated from the superior longitudinal fasciculus by the corona radiata and internal capsule.

Inferior Occipitofrontal Fasciculus (Figs 3, 5B, 6).— The inferior occipitofrontal fasciculus also connects the occipital and frontal lobes but is far inferior compared with the superior occipitofrontal fasciculus. It extends along the inferolateral edge of the claustrum, below the insula. Posteriorly, the inferior occipitofrontal fasciculus joins the inferior longitudinal fasciculus, the descending portion of the superior longitudinal fasciculus, and portions of the geniculocalcarine tract to form most of the *sagittal stratum*, a large and complex bundle that connects the occipital lobe to the rest of the brain. The middle portion of the inferior occipitofrontal fasciculus is bundled together with the middle portion of the uncinate fasciculus (see below).

Uncinate Fasciculus (Figs 3, 6, 7, 8B).—*Uncinate* is from the Latin *uncus* meaning "hook." The uncinate fasciculus hooks around the lateral fissure to connect the orbital and inferior frontal gyri of the frontal lobe to the anterior temporal lobe. The anterior aspect of this relatively short tract parallels, and lies just inferomedial to, the inferior occipitofrontal fasciculus. Its midportion actually adjoins the middle part of the inferior occipitofrontal fasciculus before heading inferolaterally into the anterior temporal lobe.

Superior Longitudinal (arcuate) Fasciculus (Figs 3, 7A, 8).—The superior longitudinal fasciculus is a mas-
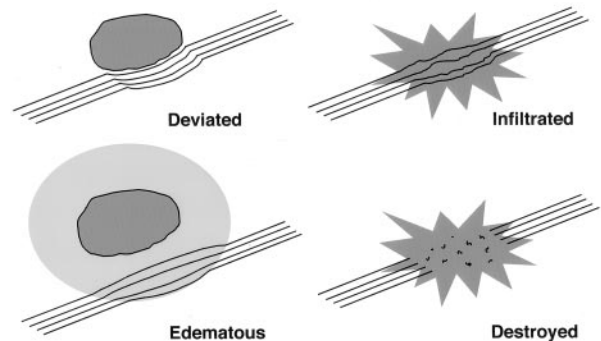
Fig 18. Potential patterns of WM fiber tract alteration by cerebral neoplasms. The extent to which these patterns can be discriminated on the basis of DTI is under investigation.

sive bundle of association fibers that sweeps along the superior margin of the insula in a great arc, gathering and shedding fibers along the way to connect frontal lobe cortex to parietal, temporal, and occipital lobe cortices. The superior longitudinal fasciculus is the largest association bundle.

Inferior Longitudinal (occipitotemporal) Fasciculus (Figs 5B and 9).—The inferior longitudinal fasciculus connects temporal and occipital lobe cortices. This tract traverses the length of the temporal lobe and joins with the inferior occipitofrontal fasciculus, the inferior aspect of the superior longitudinal fasciculus, and the optic radiations to form much of the sagittal stratum traversing the occipital lobe.
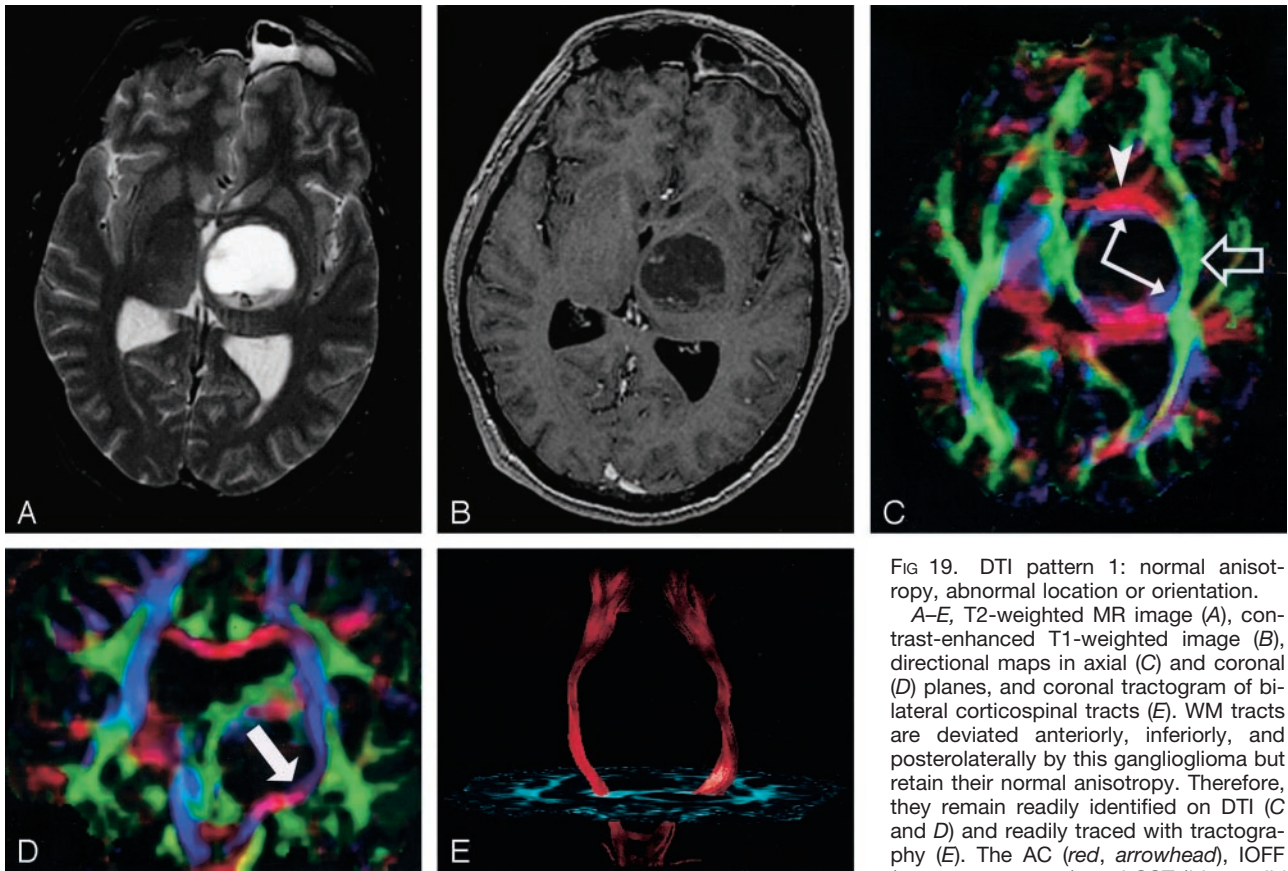
FIG 19. DTI pattern 1: normal anisotropy, abnormal location or orientation.

A–E, T2-weighted MR image (*A*), contrast-enhanced T1-weighted image (*B*), directional maps in axial (*C*) and coronal (*D*) planes, and coronal tractogram of bilateral corticospinal tracts (*E*). WM tracts are deviated anteriorly, inferiorly, and posterolaterally by this ganglioglioma but retain their normal anisotropy. Therefore, they remain readily identified on DTI (*C* and *D*) and readily traced with tractography (*E*). The AC (*red*, *arrowhead*), IOFF (*green*, *open arrow*), and CST (*blue*, *solid arrows*) are deviated. Note the blue hue of the CST change to red as it deviates toward the axial plane by the tumor (*arrow* on coronal view [*D*]).

Projection Fibers

Corticospinal, Corticopontine, and Corticobulbar Tracts (Fig 10).—The corticospinal and corticobulbar tracts are major efferent projection fibers that connect motor cortex to the brain stem and spinal cord. Corticospinal fibers converge into the corona radiata and continue through the posterior limb of the internal capsule to the cerebral peduncle on their way to the lateral funiculus. Corticobulbar fibers converge into the corona radiata and continue through the genu of the internal capsule to the cerebral peduncle where they lie medial and dorsal to the corticospinal fibers. Corticobulbar fibers predominantly terminate at the cranial motor nuclei. These bundles run together and are not discriminated on directional DTI color maps, but can be parsed by using sophisticated tractographic algorithms (21).

Corona Radiata (Fig 11).—Though not a specific tract per se, the corona radiata is one of the most easily identified structures on directional DTI color maps. Its coronally oriented fibers tend to give it a color quite distinct from that of surrounding tracts, which are oriented primarily light-right (corpus callosum) or anteroposteriorly (superior longitudinal fasciculus). Fibers to and from virtually all cortical areas fan out superolaterally from the internal capsule to form the corona radiata.

Internal Capsule (Fig 12).—The internal capsule is a large and compact fiber bundle that serves as a major conduit of fibers to and from the cerebral cortex and is readily identified on directional DTI color maps. The anterior limb lies between the head of the caudate and the rostral aspect of the lentiform nucleus, while the posterior limb lies between the thalamus and the posterior aspect of the lentiform nucleus. The anterior limb passes projection fibers to and from the thalamus (thalamocortical projections) as well as frontopontine tracts, all of which are primarily anteroposteriorly oriented in contradistinction to the posterior limb, which passes the superior-inferiorly oriented fibers of the corticospinal, corticobulbar, and corticopontine tracts. This gives the anterior and posterior limbs distinctly different colors on directional DTI maps.

Geniculocalcarine Tract (optic radiation) (Fig 13).—The optic radiation connects the lateral geniculate nucleus to occipital (primary visual) cortex. The more inferior fibers of the optic radiation sweep around the posterior horns of the lateral ventricles and terminate in the calcarine cortex; the more superior fibers take a straighter, more direct path. The optic radiation mingles with the inferior occipitofrontal fasciculus, inferior longitudinal fasciculus, and inferior aspect of the superior longitudinal

FIG 20.   DTI pattern 2: abnormal (low) anisotropy, normal location and orientation.

A–D, T2-weighted MR image (*A*), contrast-enhanced T1-weighted MR image (*B*), FA map (*C*), and directional map (*D*). The homogeneous region of hyperintensity on the T2-weighted image represents vasogenic edema surrounding a small metastasis (on another section, not shown). Despite diminished anisotropy in this region (darker region outlined on FA map) and diminished color brightness on directional map, the involved fiber tracts retain their normal color hues on the directional map (superior longitudinal fasciculus, green, arrow; corona radiata, blue, arrowhead). This preservation of normal color hues despite a substantial decrease in anisotropy is consistent with the abnormality of vasogenic edema, which enlarges the extracellular space (allowing less restricted diffusion perpendicular to axonal fibers, thus reducing the anisotropy) without disrupting cellular membranes, leaving their directional organization intact. It is not yet known to what extent this pattern is specific for edema, however.
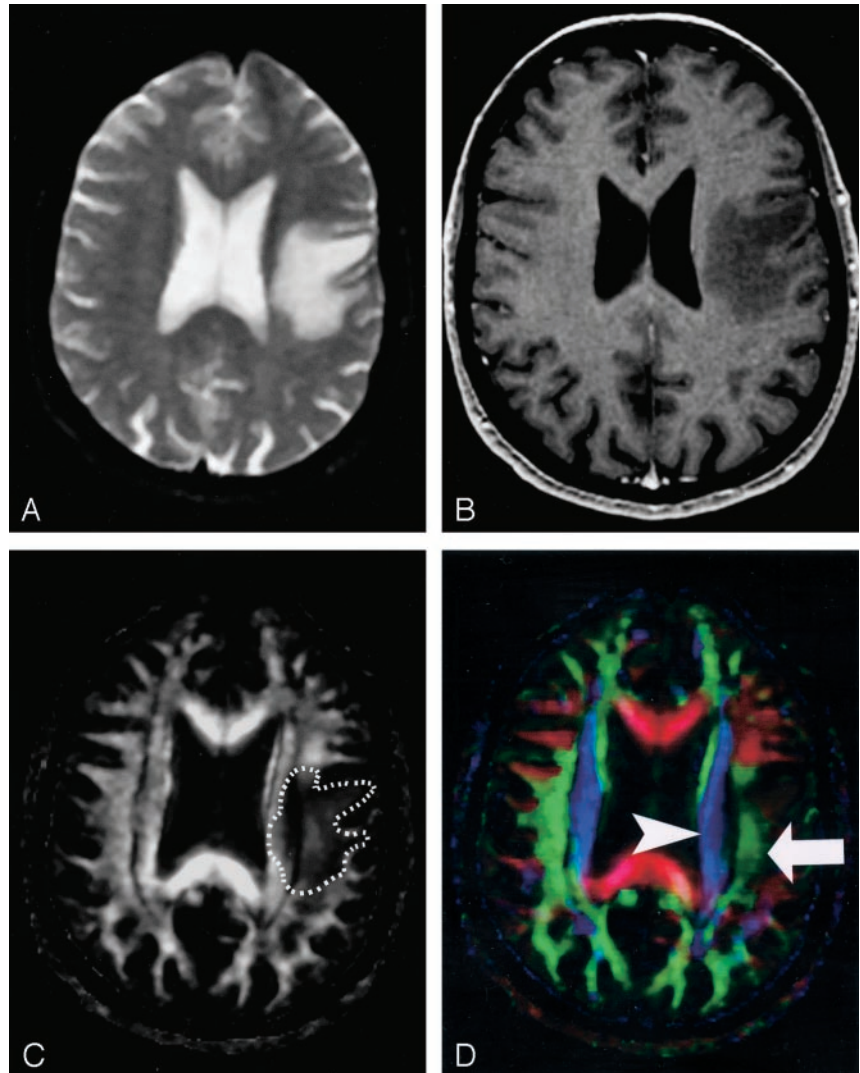
fasciculus to form much of the sagittal stratum in the occipital lobe.

Commissural Fibers

Corpus Callosum (Figs 14 and 15).—By far the largest WM fiber bundle, the corpus callosum is a massive accumulation of fibers connecting corresponding areas of cortex between the hemispheres. Fibers traversing the callosal body are transversely oriented, whereas those traversing the genu and splenium arch anteriorly and posteriorly to reach the anterior and posterior poles of the hemispheres. Near the midsagittal plane, all of the corpus callosum fibers are left-right oriented and easily identified on directional DTI color maps. However, as they radiate toward the cortex, callosal fibers interdigitate with association and projection fibers; resolving these fiber crossings with DTI is a difficult problem and the subject of intensive research (22).

Anterior Commissure (Fig 3).—The anterior commissure crosses through the lamina terminalis. Its anterior fibers connect the olfactory bulbs and nuclei;

its posterior fibers connect middle and inferior temporal gyri.

Brain Stem

The complex anatomy of the brain stem includes a large number of tracts and nuclei, as well as multiple commissures and decussations, many of which can be resolved on directional DTI color maps. Space prohibits a comprehensive review, but several commonly seen brain stem structures are illustrated in Figs 16 and 17.

DTI Patterns in WM Tracts Altered by Tumor

The goal of surgical treatment for cerebral neoplasms is to maximize the extent of tumor resection while minimizing postoperative neurologic deficits resulting from damage to intact, functioning brain. This requires preoperative or intraoperative mapping of the tumor and its relationship to functional structures, including cerebral cortex and WM tracts. Cortical mapping can be accomplished with either functional MR imaging or intraoperative electrocortical
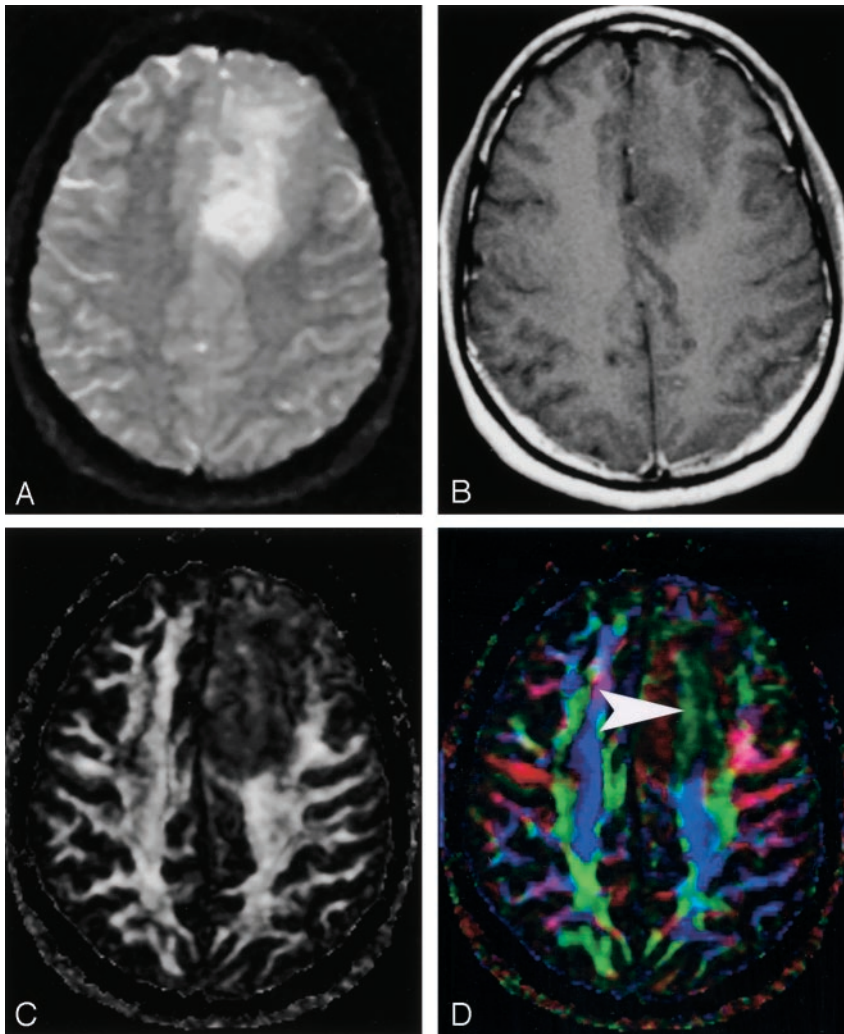
FIG 21. DTI pattern 3: abnormal (low) anisotropy, abnormal orientation.

A–D, T2-weighted MR image (*A*), contrast-enhanced T1-weighted image (*B*), FA map (*C*), and directional map (*D*). This infiltrating astrocytoma is characterized by both diminished anisotropy and abnormal color (arrowhead) on the directional map, suggesting disruption of WM fiber tract organization more severe and complex than that seen with pattern 2 (compare Fig 20). Note that the color change cannot easily be attributed to bulk mass effect as in purely deviated tracts.

stimulation. These methods are inadequate, however, for depicting the relationship of tumor to WM tracts. DTI is uniquely suited for this role.

The altered states of WM resulting from cerebral neoplasm (Fig 18) might be expected to influence the measurement of diffusion tensor anisotropy and orientation in various ways, resulting in several possible patterns on directional DTI color maps (7, 8). Intact WM tracts displaced by tumor might retain their anisotropy and remain identifiable in their new location or orientation on directional DTI color maps. Edematous or tumor-infiltrated tracts might lose some anisotropy but retain enough directional organization to remain identifiable on directional DTI maps. Finally, WM tracts might be destroyed or disrupted to the point where directional organization (and, consequently, diffusion anisotropy) is lost completely.

In a series of 20 brain tumors of various histologic diagnoses imaged preoperatively with DTI, we identified four major patterns in affected WM tracts, categorized on the basis of anisotropy and fiber direction or orientation (8).

Pattern 1 (Fig 19) consists of normal or only slightly decreased FA with abnormal location and/or direction resulting from bulk mass displacement. This is the most clinically useful pattern in preoperative planning because it confirms the presence of an intact peritumoral tract that can potentially be preserved during resection (23).

Pattern 2 (Fig 20) is substantially decreased FA with normal location and direction (ie, normal hues on directional color maps). We frequently observe this pattern in regions of vasogenic edema, although the specificity of this pattern is not yet known; further study is needed to determine the clinical utility of this observation.

Pattern 3 (Fig 21) is substantially decreased FA with abnormal hues on directional color maps. We have identified this pattern in a small number of infiltrating gliomas in which the bulk mass effect appeared to be insufficient to account for the abnormal hues on directional maps. We speculate that infiltrating tumor disrupts the directional organization of fiber tracts to cause altered color patterns on directional maps, but this phenomenon requires further study.

Pattern 4 (Fig 22) consists of isotropic (or near-isotropic) diffusion such that the tract cannot be identified on directional color maps. This pattern is observed when some portion of a tract is completely

FIG 22.   DTI pattern 4: near-zero anisotropy, tract unidentifiable.

A–D, T2-weighted MR image (*A*), contrast-enhanced T1-weighted image (*B*), FA map (*C*), and directional map (*D*). This high-grade astrocytoma has destroyed the body of the corpus callosum, rendering the diffusion essentially isotropic and precluding identification on the directional map (arrow).
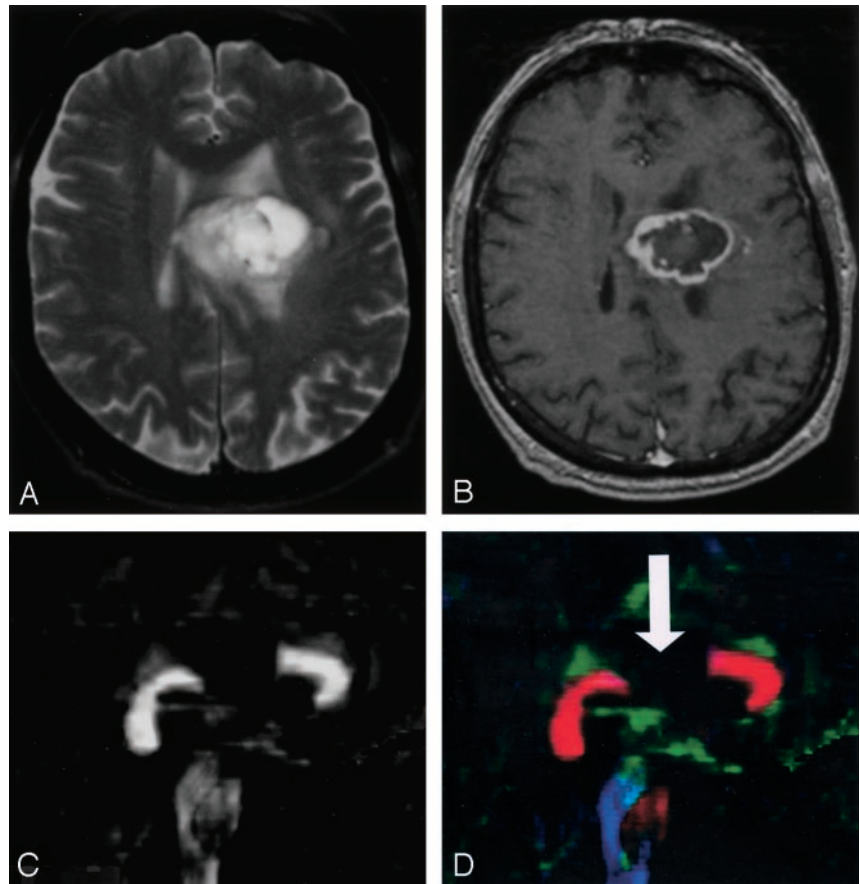
disrupted by tumor. This pattern can be useful in preoperative planning in the sense that no special care need be taken during resection to preserve a tract that is shown by DTI to be destroyed.

It should be noted that combinations of the above patterns may occur; for example, a combination of patterns 1 and 2 may be observed in a tract that is both displaced and edematous.

Summary

The polychrome produced by mapping the direction of the diffusion tensor allows rapid and unprecedented visualization of WM tracts in vivo. There is order to the complex beauty of these maps, and their interpretation requires knowledge of fiber tract anatomy that has heretofore not been commonly applied in routine clinical imaging. As DTI rapidly makes its way into the clinical realm, we have attempted to provide a concise pictorial review of the major tract anatomy typically visualized on directional DTI color maps without the more advanced and sophisticated tractographic techniques that will take somewhat longer to reach routine clinical practice. We hope this review is useful to those radiologists who already interpret DTI maps and will inspire those who have not yet incorporated DTI into their practice to do so.

References

1. Conturo TE, Lori NF, Cull TS, et al. **Tracking neuronal fiber pathways in the living human brain.** *Proc Natl Acad Sci USA* 1999;96:10422–10427
2. Mori S, Kaufmann WE, Davatzikos C, et al. **Imaging cortical association tracts in the human brain using diffusion-tensor-based axonal tracking.** *Magn Reson Med* 2002;47:215–223
3. Mamata H, Mamata Y, Westin C-F, et al. **High-resolution line scan diffusion tensor MR imaging of white matter fiber tract anatomy.** *AJNR Am J Neuroradiol* 2002;23:67–75
4. Mori S, van Zijl PCM. **Fiber tracking: principles and strategies—a technical review.** *NMR Biomed* 2002;15:468–480
5. Basser PJ, Jones DK. **Diffusion-tensor MRI: theory, experimental design and data analysis—a technical review.** *NMR Biomed* 2002; 15:456–467
6. Melhem ER, Mori S, Mukundan G, Kraut MA, Pomper MG, van Zijl PCM. **Diffusion tensor MR imaging of the brain and white matter tractography.** *AJR Am J Roentgenol* 2002;178:3–16
7. Witwer BP, Moftakhar R, Hasan KM, et al. **Diffusion-tensor imaging of white matter tracts in patients with cerebral neoplasm.** *J Neurosurg* 2002;97:568–575
8. Field AS, Alexander AL, Hasan KM, et al. **Diffusion tensor MR imaging patterns in white matter tracts altered by neoplasm.** Presented at the 10th meeting of the International Society for Magnetic Resonance in Medicine workshop on diffusion MRI biophysical issues, St. Malo, France, March 10–12, 2002.
9. Moseley ME, Cohen Y, Kucharczyk J, et al. **Diffusion-weighted MR imaging of anisotropic water diffusion in cat central nervous sys-**

tem. *Radiology* 1990;176:439–446

10. Basser PJ, Matiello J, Le Bihan D. **MR diffusion tensor spectroscopy and imaging.** *Biophys J* 1994;66:259–267

11. Papadakis NG, Murrills CD, Hall LD, Huang CL, Adrian Carpenter T. **Minimal gradient encoding for robust estimation of diffusion anisotropy.** *Magn Reson Imaging* 2000;18:671–679

12. Hasan KM, Parker DL, Alexander AL. **Comparison of gradient encoding schemes for diffusion-tensor MRI.** *J Magn Reson Imaging* 2001;13:769–780

13. Jones DK, Horsfield MA, Simmons A. **Optimal strategies for measuring diffusion in anisotropic systems by magnetic resonance imaging.** *Magn Resn Med* 1999;42:515–525

14. Sarma GN. **Leonhard Euler, the monarch of mathematicians.** *Math Education* 1972;6:B53–58

15. Basser PJ, Pierpaoli C. **Microstructural and physiological features of tissues elucidated by quantitative diffusion tensor MRI.** *J Magn Reson* 1996;111:209–219

16. Douek P, Turner R, Pekar J, Patronas N, Le Bihan D. **MR color mapping of myelin fiber orientation.** *J Comput Assist Tomogr* 1991;15:923–929

17. Woods RP, Cherry SR, Mazziotta JC. **Rapid automated algorithm for aligning and reslicing PET images.** *J Comput Assist Tomogr* 1992;16:620–633

18. Hasan KM, Basser PJ, Parker DL, Alexander AL. **Analytical computation of the eigenvalues and eigenvectors in DT-MRI.** *J Magn Reson* 2001;152:41–47

19. Lazar M, Weinstein DM, Tsuruda JS, et al. **White matter tractography using diffusion tensor deflection.** *Hum Brain Mapp* 2003;18:306–321

20. House EL, Pansky B. *A Functional Approach to Neuroanatomy.* New York: McGraw-Hill, 1960

21. Stieltjes B, Kaufmann WE, van Zijl PCM, Fredericksen K, Pearlson GD, Mori S. **Diffusion tensor imaging and axonal tracking in the human brainstem.** *Neuroimage* 2001;14:723–735

22. Wiegell MR, Larsson HBW, Wedeen VJ. **Fiber crossing in human brain depicted with diffusion tensor MR imaging.** *Radiology* 2000;217:897–903

23. Alexander AL, Badie B, Field AS. **Diffusion tensor MRI depicts white matter reorganization after surgery (abstr).** In: *Proceedings of the 11th Meeting of the International Society of Magnetic Resonance in Medicine 2003.* Berkeley, CA: International Society for Magnetic Resonance in Medicine, 2003:399